Sound Velocity in Heat Transfer Salt (Mixture of Molten $NaNO_3$–KNO_3–$NaNO_2$, 7/44/49 mol %) Studied by an Ultrasonic Pulse–Echo Method

Masuhiro Mikami, Osamu Odawara,† and Kazutaka Kawamura*

Research Laboratory for Nuclear Reactors, Tokyo Institute of Technology, O-okayama, Meguro-ku, Tokyo 152, Japan

The velocity of sound in HTS (heat transfer salt; $NaNO_3$–KNO_3–$NaNO_2$, 7/44/49 mol %) is measured by means of an ultrasonic pulse–echo method over a wide range of temperature. The results are expressed as a function of temperature by $u = 2040 - 1.323(T - 415)$ at 450–693 K. The adiabatic compressibility and the isochoric specific heat are calculated from the present results and the existing data on the density and the isobaric specific heat. Similar measurements are carried out for molten $NaNO_2$, $NaNO_3$, and KNO_3; molten $NaNO_3$ and KNO_3 are the salts whose data on sound velocity and related properties are widely available.

Introduction

The available information on sound velocity in molten salts is of importance in both studying the basic molecular processes in transport phenomena and giving direct or indirect information to technical applications at elevated temperatures. Although a number of methods have been proposed for the measurement of sound velocity in liquids such as continuous-wave techniques (*1*), sing-around methods (*2*), ultrasonic-pulse methods (*3*), and optical methods (*4*), there exist few methods to give reliable information on sound velocity in molten salts. The measurements in molten salts are more difficult than the corresponding measurements at room temperature because of the corrosion of supporting materials and the temperature drift at high-temperature operations.

For the measurement of propagation of sound in solids, an ultrasonic pulse–echo method has widely been used (*5*). When the ultrasonic pulse–echo method is applied to the measurement of molten salts, it has some advantages compared with other methods; only one quartz rod is needed as a conductor of sound waves, which reduces temperature gradients in the material tested, and the parallelism between the planes of the conductor and the reflector can be controlled more easily.

The heat-transferring material HTS is useful for practical purposes, since it is stable over a relatively wide range of temperature (450–850 K) and its heat transfer coefficient is large (6). Reliable data on propagation of sound for this material are indispensable for making clear the structure and transport mechanism in molten nitrate mixtures. In the present work, the sound velocity in HTS was measured over a wide range of temperature by means of an ultrasonic pulse–echo method, and the adiabatic compressibility and the isochoric specific heat were calculated from the present results and the existing data on the density and the isobaric specific heat. The sound velocities in molten $NaNO_3$ and KNO_3 were measured to check this method, and that in $NaNO_2$ was also measured.

Experimental Section

In the present work an ultrasonic pulse–echo method was applied to the measurement of sound velocity in molten salts. The schematic design of the apparatus is shown in Figure 1.

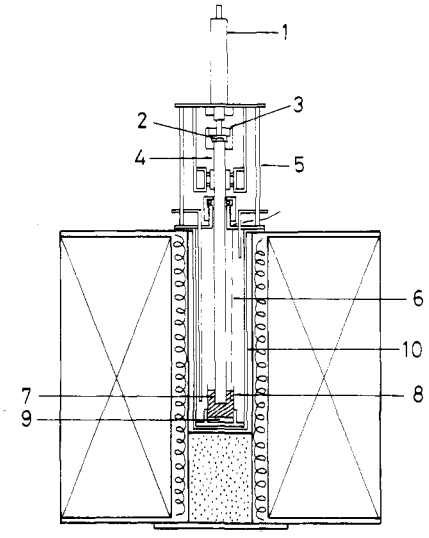

Figure 1. Schematic diagram of the apparatus used for an ultrasonic pulse–echo method: (1) micrometer, (2) X-cut quartz crystal transducer, (3) bearing, (4) conductor, (5) leveling screws, (6) thermocouple, (7) molten salt, (8) cell, (9) reflector, (10) stainless-steel vessel.

An X-cut quartz crystal transducer (15 MHz) was attached to a quartz rod as a conductor with phenyl salicylate. The rod was of optical quality, and its dimensions were optimized for getting the maximum detectibility of the pulse and the time interval between echoes; the diameter was 12 mm and the length was 370 mm. The conductor was fixed to a holder with a bearing, which was connected to a micrometer. The transducer was cooled by circulating water around the holder. The ultrasound was transmitted through the conductor into the tested salt within the cell and reflected at the bottom plate of the cell. The parallelism between the planes of the conductor and the reflector was adjusted with the leveling screws to get suitable echo patterns. The reflection pattern was monitored on an oscilloscope. The time interval was recorded within 0.01 μs. The distance between the planes of the conducting rod and the bottom plate was adjusted by the micrometer with an accuracy of ± 5 μm. The molten salts were blanketed with dried argon, and the temperature was controlled to within 1 K. The pulse–echo time intervals were measured at successive 2-mm separation intervals of the planes between the conductor and the reflector, up to $\sim$40 mm. Varied path lengths were used to reduce errors arising from nonparallelism of the major reflecting planes and from spurious reflections.

Sound velocities in H_2O, $NaNO_3$, KNO_3, $NaNO_2$, and HTS were measured. For $NaNO_2$, it was not possible to measure at more than 590 K because of thermal decomposition. All of the chemicals were of analytical reagent grade. HTS was prepared by weighing accurately and mixing the three salts ($NaNO_3$, KNO_3, and $NaNO_2$), which had been fully dried. The ratio of the constituent cations, Na^+ and K^+, was checked by flame spectrophotometry, and that of NO_2^- by iodometric titration. The volume of the liquids needed for the measurement of sound velocity was $\sim$35 mL.

† Present address: Government Industrial Research Institute, Tohoku, Haranomachi, Sendai 983, Japan.

0021-9568/81/1726-0411$01.25/0

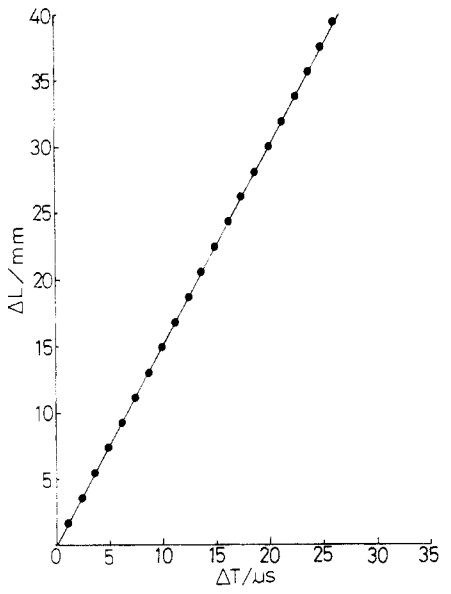

Figure 2. Relationship between the path length ΔL and the delay time ΔT for a typical experiment in distilled water at 303 K.

Table I. Experimental Data for Molten $NaNO_3$, KNO_3, $NaNO_2$, and HTS

salt	temp, K	u, m s^{-1}	$10^{11}\beta_s$, m^2 N^{-1}	γ	C_v, J mol^{-1} K^{-1}
$NaNO_3$	609	1763.3	17.07[a]	1.149[a]	135.3[a]
	625	1751.5	17.40	1.153	134.8
	638	1737.3	17.78	1.155	134.6
	646	1726.8	18.05	1.156	134.4
	667	1707.0	18.62	1.160	134.0
	695	1680.6	19.42	1.165	133.4
	705	1671.9	19.70	1.167	133.2
KNO_3	625	1740.1	17.76[b]	1.237[b]	100.2[b]
	627	1737.9	17.82	1.238	100.1
	650	1705.8	18.67	1.242	99.8
	677	1676.9	19.52	1.249	99.2
	705	1640.5	20.63	1.254	98.8
	713	1638.4	20.75	1.258	98.5
$NaNO_2$	565	1876.8	15.73[c]	1.195[c]	100.9[c]
	567	1870.5	15.85	1.194	101.0
	571	1868.9	15.91	1.196	100.8
	578	1855.5	16.18	1.197	100.7
	581	1850.8	16.29	1.197	100.7
	583	1848.8	16.33	1.198	100.6
	585	1846.6	16.39	1.198	100.6
	586	1845.9	16.41	1.199	100.5
HTS	450	1990.5	12.91[d]	1.158[d]	117.8[d]
	458	1973.1	13.18	1.159	117.7
	478	1958.2	13.48	1.166	117.0
	491	1950.8	13.65	1.171	116.5
	501	1930.6	13.99	1.172	116.4
	505	1929.2	14.04	1.174	116.2
	524	1892.4	14.69	1.176	116.0
	531	1880.3	14.92	1.177	115.9
	552	1861.0	15.36	1.183	115.3
	585	1813.2	16.39	1.189	114.8
	609	1782.5	17.12	1.194	114.3
	626	1767.5	17.53	1.199	113.8
	641	1740.1	18.19	1.200	113.7
	648	1730.6	18.45	1.201	113.6
	660	1715.9	18.85	1.203	113.4
	693	1671.0	20.15	1.208	113.0

[a] Calculated with $\rho = 2.320 - (0.715 \times 10^{-3})T$ g cm^{-3} (*7*) and $C_p = 155.4$ J mol^{-1} K^{-1} (*7*). [b] Calculated with $\rho = 2.315 - (0.729 \times 10^{-3})T$ g cm^{-3} (*7*) and $C_p = 123.9$ J mol^{-1} K^{-1} (*7*). [c] Calculated with $\rho = 2.226 - (0.746 \times 10^{-3})T$ g cm^{-3} (*7*) and $C_p = 120.5$ J mol^{-1} K^{-1} (this work). [d] Calculated with $\rho = 1.980 - (0.729 \times 10^{-3})(T - 415)$ g cm^{-3} (*6*) and $C_p = 136.5$ J mol^{-1} K^{-1} (*6*).

Table II. Expressions for Sound Velocities in Molten $NaNO_3$, KNO_3, $NaNO_2$, and HTS as a Function of Temperature

salt	u, m s^{-1}	temp range, K	ref
$NaNO_3$	$2478 - 1.150T$	583–723	*8*
	$2490 - 1.155T$	583–722	*9*
	$2618.7 - 1.6291T + (4.2426 \times 10^{-4})T^2$	*a*	*10*
	$2354.0 - 0.968T$	609–705	this work
KNO_3	$2483 - 1.194T$	593–803	*8*
	$2450 - 1.12T$	609–712	*9*
	$2766.3 - 1.9149T + (4.6856 \times 10^{-4})T^2$	*a*	*10*
	$2480.7 - 1.187T$	625–713	this work
$NaNO_2$	$2706.1 - 1.470T$	565–586	this work
HTS	$2589.3 - 1.323T$	450–693	this work

[a] Unspecified in the literature.

Results

The time interval between echoes varied linearly with the position of the conducting rod. The sound velocity was determined from the slope of the relative path length, ΔL, vs. the time interval, ΔT, between echoes. The relationship between ΔL and ΔT is shown in Figure 2 for the typical measurement of distilled water. The sound velocity in distilled water was determined as 1511 ± 3 m s^{-1} at 303 K from a least-squares fit to the data.

The sound velocities in $NaNO_3$, KNO_3, $NaNO_2$, and HTS obtained in the present work are tabulated in Table I. The adiabatic compressibility and the isochoric specific heat were calculated from the present results as follows:

$$\beta_s = 1/\rho u^2$$

$$C_p/C_v = \gamma = 1 + u^2\alpha^2 MT/C_P$$

The data on ρ, α, and C_p of $NaNO_3$, KNO_3, KNO_3, and $NaNO_2$ were taken from ref *7* except C_p of $NaNO_2$. Since C_p of $NaNO_2$ is not in the literature, the value was measured with a DSC instrument (Perkin-Elmer Model DSC-2) and found to be 120.5 J mol^{-1} K^{-1} at 565–583 K. The data for HTS were taken from ref *6*. The calculated values of β_s, γ, and C_v are also tabulated in Table I.

The sound velocities in molten $NaNO_3$, KNO_3, $NaNO_2$, and HTS were fitted by least squares to functions of temperature and tabulated in Table II. The equations are compared with those previously determined (*8–10*) on molten $NaNO_3$ and KNO_3.

Discussion

Since the sound velocity in distilled water measured in the present work is consistent with the recommended value measured by a sing-around method (*11*), 1509.4 m s^{-1} at 303 K, within experimental error; the present method is considered reliable at least at room temperature. The main sources of error in the present work are in measuring the time interval (~0.1%) and the path length (~0.05%), so that most experiments were performed within 0.2% of experimental errors.

As shown in Table II, the sound velocities in molten $NaNO_3$ and KNO_3 measured in the present work are in good agreement with the literature values although the temperature dependence is a little different. When the results for HTS were compared with those for each component, the sound velocity in HTS was found to be almost the same as the value of the additive sum of $0.07u_{NaNO_3}$, $0.44u_{KNO_3}$, and $0.49u_{NaNO_2}$, i.e., $2038 - 1.310(T - 415)$. This might mean that the association of the components in HTS is not significant for the propagation of sound in HTS.

As can be seen from Table I, the calculated values of β_s and C_v are in the following order, although the temperature range

of measurement for $NaNO_2$ is a little narrow:

$$\beta_{s,KNO_3} > \beta_{s,NaNO_2} > \beta_{s,HTS} > \beta_{s,NaNO_3}$$

$$C_{v,NaNO_3} > C_{v,HTS} > C_{v,NaNO_2} > C_{v,KNO_3}$$

The sound velocity in $NaNO_3$ is greater than that in KNO_3 and conversely for β_s, while in $NaNO_2$ both u and β_s are greater than those of $NaNO_3$. Since the size of the cation is smaller in $NaNO_3$ than in KNO_3, the coordination in the structure would make the sound velocity in $NaNO_3$ greater than in KNO_3. For $NaNO_2$, the librational contribution between cation and anion becomes more important than for $NaNO_3$ from the structural difference of the anion, and this causes the sound velocity in $NaNO_2$ to be greater than that in $NaNO_3$ although $\beta_{s,NaNO_2}$ is greater than $\beta_{s,NaNO_3}$.

Glossary

u	sound velocity, m s^{-1}
T	temperature, K
ΔL	change in distance between the conductor and the reflector, m
ΔT	change in time interval, s
β_s	adiabatic compressibility, m^2 N^{-1}
ρ	density, g cm^{-3}
C_p	isobaric specific heat, J mol^{-1} K^{-1}
C_v	isochoric specific heat, J mol^{-1} K^{-1}
α	thermal expansivity, K^{-1}
M	molar volume

Literature Cited

(1) Fox, F. E. *Phys. Rev.* **1937**, *52*, 973.
(2) Hanson, R. L. *J. Acoust. Soc. Am.* **1949**, *21*, 60.
(3) Pellam, J. R.; Galt, J. K. *J. Chem. Phys.* **1946**, *14*, 608.
(4) Selfen, N. *Z. Phys.* **1938**, *108*, 681.
(5) Roderick, R. L.; Truell, R. *J. Appl. Phys.* **1952**, *23*, 267.
(6) Kirst, W. E.; Nagle, W. M.; Castner, J. B. *Trans. Am. Inst. Chem. Eng.* **1940**, *36*, 371.
(7) Janz, G. J. "Molten Salts Handbook"; Academic Press: New York, 1967; pp 42, 200.
(8) Bockris, J. O'M.; Richards, N. E. *Proc. R. Soc. London, Ser. A* **1957**, *241*, 44.
(9) Higgs, R. W.; Litovitz, T. A. *J. Acoust. Soc. Am.* **1960**, *32*, 1108.
(10) Cerisier, P.; Finiels, G.; Doucet, Y. *J. Chim. Phys.* **1974**, *6*, 836.
(11) Greenspan, M.; Tschiegg, C. E. *J. Acoust. Soc. Am.* **1959**, *31*, 75.

Received for review November 21, 1980. Accepted June 12, 1981.

Isobaric Binary Vapor–Liquid Equilibria for the Systems Allyl Alcohol–Toluene and Toluene–Benzaldehyde

K. Venkateswara Rao,* A. Raviprasad, and C. Chiranjivi

Department of Chemical Engineering, Andhra University, Visakhapatnam 530003, India

Isobaric vapor–liquid equilibria for the binary systems allyl alcohol–toluene and toluene–benzaldehyde were measured at 760 ± 1 mmHg pressure by using a modified Jones vapor recirculatory still. The system allyl alcohol–toluene has shown positive deviations from Raoult's law. Redlich–Kister, Wilson, NRTL, and UNIQUAC models were employed to correlate the experimental data. The system toluene–benzaldehyde was nearly ideal in its behavior, and the data were correlated by the method of Hirata.

Isobaric vapor–liquid equilibrium (VLE) data at 760 ± 1 mmHg pressure were determined for the systems allyl alcohol–toluene and toluene–benzaldehyde. The VLE data of the former system find use in the purification of allyl alcohol. Toluene–benzaldehyde mixtures occur in the manufacture of benzaldehyde from toluene. Hence, knowledge of vapor–liquid equilibrium data on these systems is of use in the design of separation equipment. The VLE data on allyl alcohol–toluene mixtures at 760-mmHg pressure and at 90 °C were reported in the literature (*1*, *2*).

Experimental Section

Purity of Chemicals. Analytical-grade allyl alcohol and toluene were distilled in a Defton column, and the middle fractions were collected and used. Benzaldehyde, also of analytical grade, was distilled under vacuum, and the heart cuts of the distillate were used in the experimental runs. The physical constants of the pure components, compared with the literature values (*3*), are presented in Table I along with the source of the chemicals. Special care was taken to see that benzaldehyde did not come in contact with oxygen in the air during the distillation and use in the equilibrium still by connecting an alkaline pyrogallol tower to the system to prevent atmospheric oxidation of benzaldehyde.

Apparatus, Technique, and Analysis. The VLE data were measured by using the Jones vapor recirculatory still modified by Ward (*4*). The operation of the still was described previously (*5*). Vapor condensate and liquid-phase samples were analyzed by precision refractometry (Abbe's refractometer) at 30 ± 0.1 °C with the aid of calibration curves constructed from n_D vs. x data measured for synthetic binary mixtures. The equilibrium temperatures were taken with a mercury-in-glass thermometer having an accuracy of ±0.1 °C. The estimated precision of the equilibrium mixture composition measurements was ±0.006 mole fraction for allyl alcohol–toluene mixtures and ±0.01 mole fraction for toluene–benzaldehyde mixtures.

Results and Discussion

The vapor–liquid equilibrium data for the two systems studied are given in Tables II and III.

The liquid-phase activity coefficients for each component were calculated from the experimental data by using eq 1. At

$$\gamma_i = \Pi\phi_i^v y_i/(P_i^s \phi_i^s x_i) \quad (1)$$

atmospheric pressure, the ratio ϕ_i^v/ϕ_i^s was found to be around unity. Hence, it was ignored in the calculations. This is in

0021-9568/81/1726-0413$01.25/0